Global Mean Sea Level Variation On Interannual-Decadal Timescales: Climatic Connections

Jennifer Ting-Juan Liao
National Taiwan University https://orcid.org/0000-0003-3555-919X
Benjamin Fong Chao (bfchao@earth.sinica.edu.tw)
Institute of Earth Sciences, Academia Sinica

Research Letter

Keywords: Global mean sea level, Interannual, Decadal, Correlation, Climatic Oscillations

Posted Date: November 4th, 2021

DOI: https://doi.org/10.21203/rs.3.rs-1036015/v1

Global Mean Sea Level Variation on Interannual-Decadal Timescales: Climatic Connections

J. T. Liao[1], B. F. Chao[2]*

[1]Department of Physics, National Taiwan University, Taipei, Taiwan

[2]Institute of Earth Sciences, Academia Sinica, Taipei, Taiwan

* Corresponding address: bfchao@earth.sinica.edu.tw

Abstract.

We investigate the influences of the climatic oscillations on global mean sea level (GMSL) on interannual-decadal (ID) timescales. We conduct correlation analyses on the GMSL-ID time series, which is obtained upon removing numerically the long-term trend and seasonal variations from satellite radar altimeter data since 1992, with several climatic oscillations represented by their respective meteorological indices, including El Niño-Southern Oscillation (ENSO), Pacific Decadal Oscillation (PDO), Atlantic Multidecadal Oscillation (AMO), Arctic Oscillation (AO), Antarctic Oscillation (AAO). From the time-domain correlation and frequency-domain coherence, we find: (i) High correlation between GMSL-ID and ENSO concentrated on the Central-Pacific type of ENSO on timescales longer than 1.5 years primarily, but essentially no correlation with the eastern Pacific type of ENSO. (ii) Moderate correlations of GMSL-ID with the long-period undulation of PDO on timescales of over 4 years, and with AMO on timescale of 2-10 years with AMO leading in phase to GMSL-ID by 8 months. (iii) Weak correlation of GMSL-ID (here indicating water exchange with the Arctic as our GMSL-ID data actually do not cover Arctic sea) with AO. (iv) Practically no correlation between GMSL-ID and AAO. Finally, we least-squares fit the above five indexes to GMSL-ID to assess the relative contribution of each oscillation in causing the observed GMSL-ID, for a better understanding of the GMSL under the influences of the on-going climate changes.

Keywords

Global mean sea level, Interannual, Decadal, Correlation, Climatic Oscillations

1. Introduction

The sea level varies with time anywhere in the ocean on all timescales for a myriad of reasons. Conventional tide gauges monitor long-term sea level but only relative to the local ground at sparse coastal sites. Modern satellite radar altimetry on the other hand measures absolute sea level in the terrestrial reference frame uniformly over open oceans on global scales. One important product has been the averaged global mean sea level (GMSL) anomaly as a continuous single time series referenced to the time-mean value.

In terms of time dependence, the most prominent variations in the GMSL are the secular sea-level rise and the seasonal fluctuations. A subject of active research, the secular rise is a consequence of the global warming in the form of thermal expansion of the surface water and additional water inflow from land; the latter includes melting glaciers and ice-sheets, modified by anthropogenic effects of artificial-dam water impoundment and groundwater discharge (e.g., Cazenave et al., 2018; Frederikse et al., 2020). The seasonal signals follow the climatology of water exchanges of the ocean with land and atmosphere plus steric variations (e.g., Chen et al., 2005; Vinogradov et al., 2008; Garcia-Garcia et al., 2020).

In this paper we turn attention and target the non-secular and non-seasonal variability of GMSL on the interannual-to-decadal timescale, henceforth referred to as GMSL-ID. Studying the GMSL-ID, which reflects processes of the global water cycle that are related to climate variabilities (cf. Cazenave and Remy, 2011), is a scientific pursuit toward better understanding and monitoring of the on-going climatic changes. Evidences of such connections have been reported on specific basis especially with respect to extreme events. For example, Chambers et al. (2002) detected signature of El Ninos in GMSL along with certain 10~12-year variabilities. Willis et al. (2008) examined the anomalous GMSL budget during 2004-2005. Boening et al. (2012) found unequivocal link of GMSL with the strong 2011 La Nina event of the El Nino/Southern Oscillation (ENSO) which retained a great amount of water on land lowering the GMSL by as much as 5 mm. Cazenave et al. (2012) and Haddad et al. (2013) assessed the influence of ENSO and identified signatures of several El Nino/La Nina episodes in GMSL. Jin et al. (2012) and Zhang and Church (2012) reported possible connections of Pacific sea level variations with ENSO and Pacific Decadal Oscillation (PDO); Hamlington et al. (2013; 2017) found significant contribution of PDO to GMSL; Kuo et al. (2021) contrasted the influence of two different El Ninos on GMSL. Conversely, Wahl and Chambers (2016) and Rohmer and Le Cozannet (2019) made statistical studies on GMSL's connection and impacts on extreme climatic events.

In the present paper we aim to "explain" GMSL-ID following the approach of Chao et al. (2020) in understanding the variations in Earth's oblateness J_2. We shall assess and quantify the contributions

of the major climatic oscillations in the ocean-atmosphere system to the observed GMSL-ID, and do so via correlation investigations in both time- and frequency-domains.

2. Data Preparations and Methodology

Several versions of the GMSL time series have been solved by different agencies based on different treatments of systematic corrections in the satellite altimetry observation. Figure 1(a) presents the GMSL time series that we shall use, courtesy of U. Colorado. It is obtained by averaging the sea level height between 66°S and 66°N (on account of the orbit inclination of the Topex/Jason satellite series, covering about 95% of the world's ice-free ocean area), at sampling interval of 10 days (Topex/Jason's orbit repeat cycle); the timespan is from 1992.9 (Topex's launch year) to 2020.75.

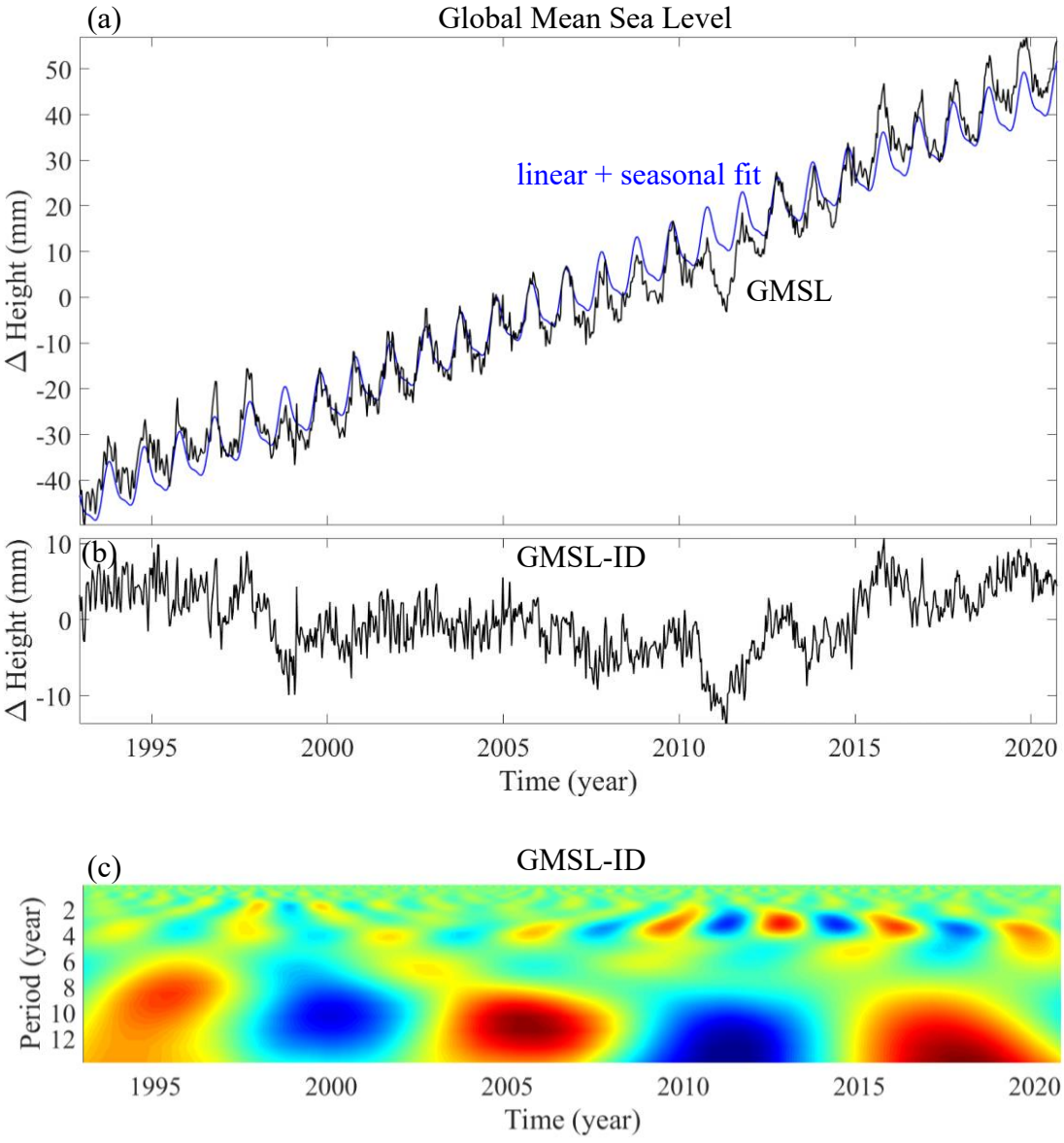

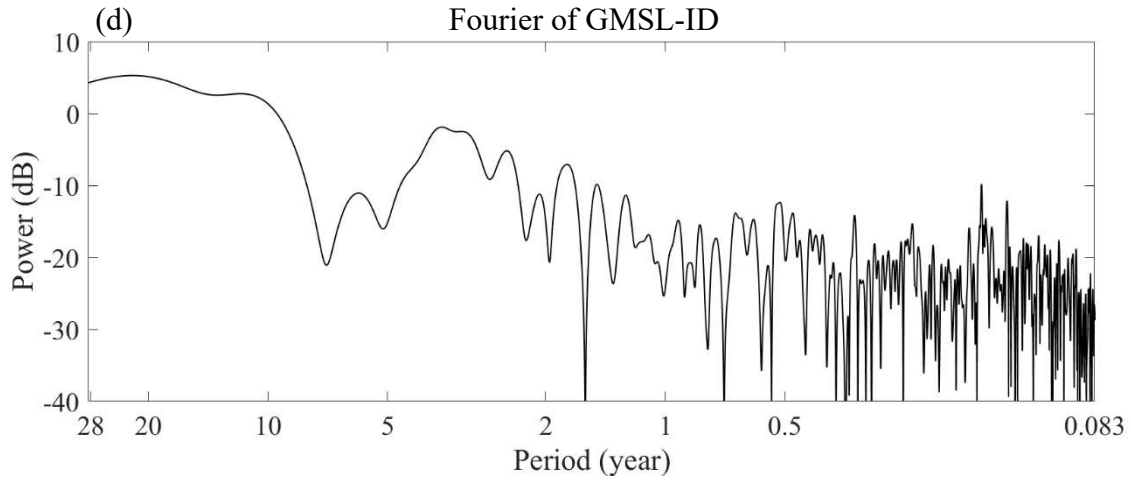

Figure 1. Time series of the altimetry-observed global mean sea level (GMSL), 1992.9 - 2020.75. (a) The original GMSL data (black) overlaid with the least-squares fit of a linear + seasonal (annual + semi-annual) terms. (b) The interannual-decadal GMSL-ID time series, i.e. the difference between the two curves in (a); note the different scales. (c) Time-frequency Morlet wavelet spectrum of GMSL-ID in (b) on interannual-decadal timescale. (d) Fourier power spectrum of GMSL-ID, plotted as a function of logarithmic of frequency to accentuate the lower-frequency portion.

We first model the GMSL time series as a linear combination of various numerical terms:

$$\text{GMSL}(t) = a + bt + c\,\sin\omega t + d\,\cos\omega t + e\,\sin 2\omega t + f\,\cos 2\omega t + \text{GMSL-ID}(t), \qquad (1)$$

where angular frequency $\omega = 2\pi/(365.25 \text{ days})$. The term $a + bt$ is to represent the secular sea-level rise in the form of the mean + linear trend, while the four sinusoidal terms account for the seasonality at annual and semi-annual periods. The coefficients a, b, …, f are then solved by linear least-squares regression on the GMSL(t) data (Figure 1a) by minimizing the variance of the residual, which is our target GMSL-ID(t). The fit estimates are: the linear rate of sea-level rise is b = 3.28 mm/year; the annual amplitude 5.3 mm peaks around October 26; semiannual amplitude 1.6 mm peaks around January 2. Their sum, shown as the overlay in Figure 1(a), not surprisingly accounts for the bulk of the GMSL variability.

Figure 1(b) then gives the broad-band residual GMSL-ID(t), upon de-trend/de-season of GMSL, i.e. removing the secular trend and the seasonality. Figure 1(c) gives the time-frequency (Morlet) wavelet spectrum of GMSL-ID(t) (e.g., Chao et al., 2020), where two quasi-periodic signals stand out: one around 4 years growing in strength after ~2005, and one around 10.5 years which only sees ~2.5 cycles as limited by the data timespan. Figure 1(d) gives the Fourier power spectrum of GMSL-ID(t), whereof the red nature of the power is evident.

The major climatic oscillations that we shall examine with respect to GMSL-ID are: ENSO, PDO, Atlantic Multi-decadal Oscillation (AMO), Antarctic Oscillation (AAO), and Arctic Oscillation (AO). As typical, the strength of a given climatic oscillation is represented by its (dimensionless) index on a continuous time basis, whereof the complexities associated with the oscillation have been optimally blended into one single time series. The said Index time series at monthly intervals are plotted in Figure 2, along with their respective wavelet spectra on the interannual-decadal timescale.

ENSO is the most prominent climate oscillation pattern involving changes in the water temperature and air pressure in the tropical Pacific Ocean; the MEI (Multivariate ENSO Index) used here is the first unrotated principal component of six main observed climatic variables over the tropical Pacific. Here we further distinguish (see below) two types of ENSO that differ in their regional extents as well as timing with respect to seasonality: the ENSO-EP (Eastern Pacific) type and the ENSO-CP (Central Pacific) type. Their indices are defined by the principal component of the sea surface temperature in the Pacific, ENSO-EP excluding the Nino-1 region and ENSO-CP excluding the Nino-4 region (Kao and Yu, 2009). ENSO-CP became more prominent against ENSO-EP since the 21st century, for example the El Nino-CP event in 2012.

The PDO Index is defined as the leading principal component of the monthly mean sea-surface temperature variability over the North Pacific sector in the region poleward of 20°N.

The AMO is a coherent mode of natural variability based upon the average anomalies of sea surface temperatures, with AMO Index to reflect the non-secular multi-decadal sea-surface temperature pattern variability in in the North Atlantic basin.

The AAO (also known as the Southern Annular Mode) describes the intensity of the westerly wind jet surrounding the Antarctic, quantified by the AAO Index which is the leading principal component of the 700 hPa atmospheric geopotential height anomalies poleward of 20°S.

Counterpart to AAO, the AO (also known as the Northern Annular Mode) is closely related to and encompassing the conventional North Atlantic Oscillation (NAO; Wallace & Gutzler, 1981). It is to be interpreted as the surface signature of modulations in the strength of the polar vertex aloft the Arctic (Thompson & Wallace, 2000), while the AO Index is constructed by projecting the 1000 hPa height anomalies poleward of 20°N.

Despite the difference in their primary timescales, PDO and ENSO carry considerable correlation between their conventional indices because of the geographical juxtaposition in the Pacific Basin; for example, they show corresponding decadal behaviors evident in their wavelet spectra in Figure 2. Wanting mathematical orthogonality, that makes identifying the individual contributions to GMSL troublesome. Therefore in the processing to be conducted below we take the filtered version of the indices to accentuate the signal frequency contents as follows: the Indices of ENSO, ENSO-CP, ENSO-EP are high-pass filtered at the period of 8 years (see Figure 2 a, b, c, the blue curves), whereas the PDO Index low-pass filtered at 8 years (Figure 2d).

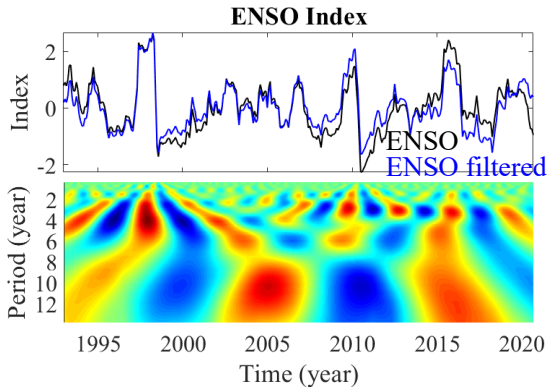
ENSO Index
Index
ENSO
ENSO filtered
Period (year)
Time (year)

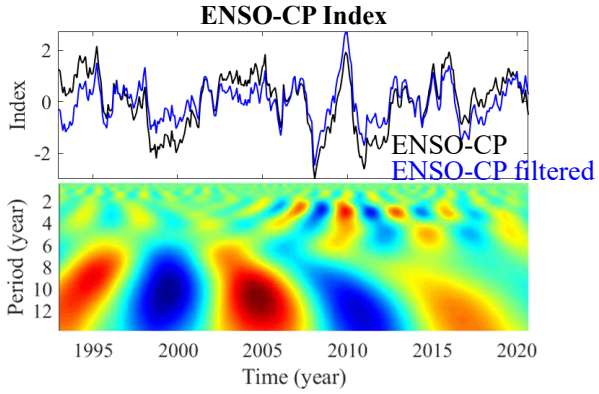
ENSO-CP Index
Index
ENSO-CP
ENSO-CP filtered
Period (year)
Time (year)

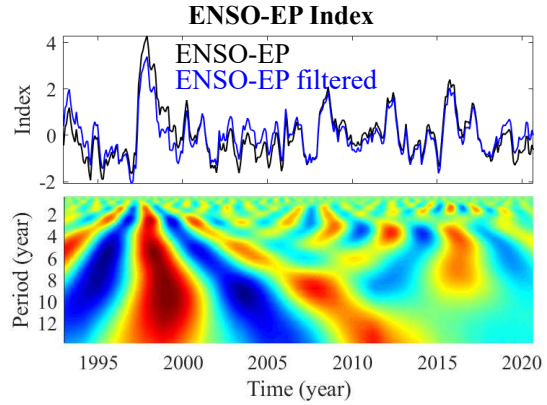
ENSO-EP Index
Index
ENSO-EP
ENSO-EP filtered
Period (year)
Time (year)

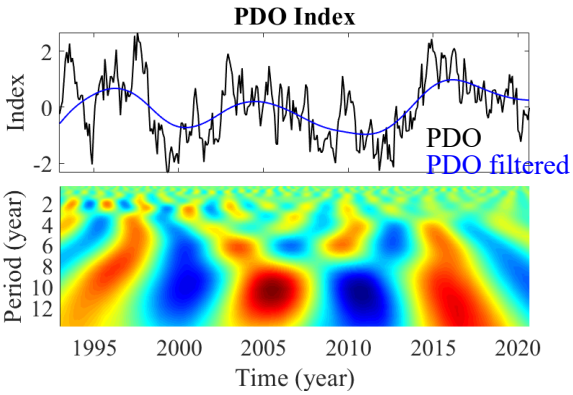
PDO Index
Index
PDO
PDO filtered
Period (year)
Time (year)

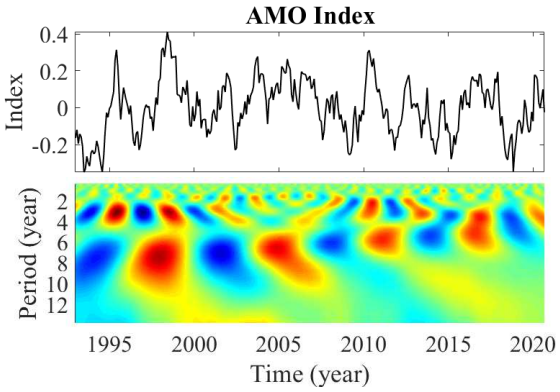
AMO Index
Index
Period (year)
Time (year)

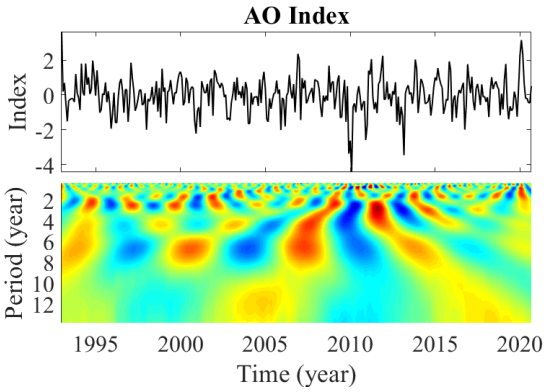
AO Index
Index
Period (year)
Time (year)

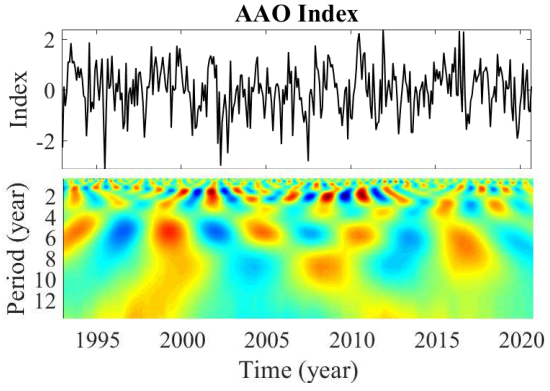
AAO Index
Index
Period (year)
Time (year)

Figure 2. Time series of the various climatic oscillation Indices used in this study and their time-frequency (Morlet) wavelet spectra. (Blue curves are the high- or low-pass filtered versions; see text.)

The GMSL-climate connection is to be investigated via correlation analyses. In the time domain we calculate the linear cross-correlation function as a function of relative time shift between the two data series. The obtained correlation values are assessed against the statistical degrees of freedom (e.g., Chao & Chung, 2019). Correspondingly one can further delineate how the found correlations break down in terms of timescale according to the (complex) cross-coherence spectra in the frequency domain. In evaluating the coherence we adopt the algorithm of Chao & Eanes (1995), where seven orthogonal multi-tapers (Thomson, 1982) with time-bandwidth product of 4π are employed for the spectral averaging; again, the confidence level is assessed against the associated degree of freedom (Chao & Chung, 2019).

3. Results for GMSL-Climate Correlation

We conduct the correlation analyses of GMSL-ID(t) with respect to the Indices of the afore-mentioned climatic oscillations in Figure 2. Figure 3 shows the time-domain cross-correlation functions, as functions of relative time shift (in months) where positive time shift means the oscillation leading GMSL-ID(t) in phase. Figure 4 shows the corresponding frequency-domain coherence spectra. We shall discuss these results in Section 4.

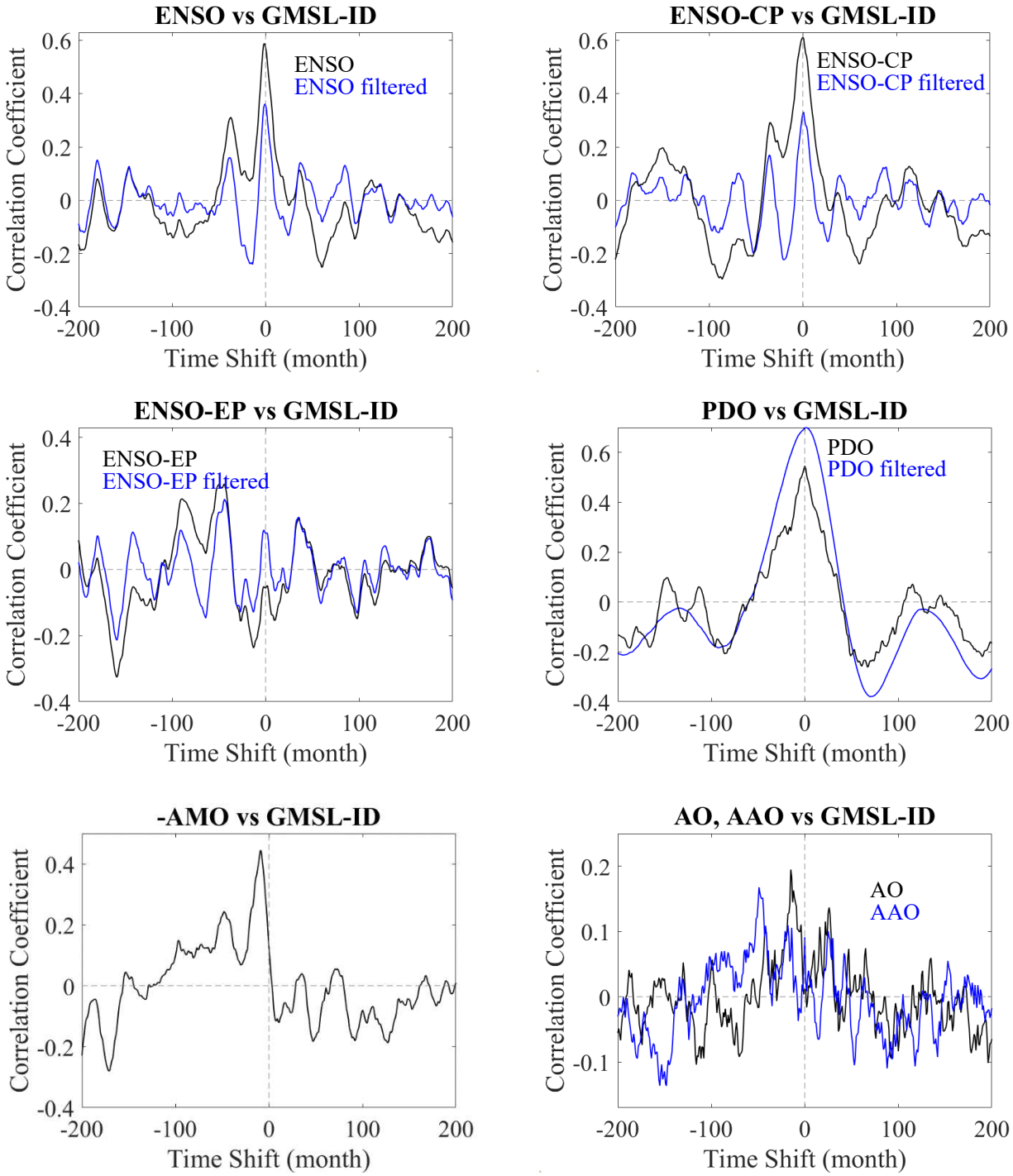

Figure 3. time-domain cross-correlation functions of GMSL-ID(t) w.r.t. the Indices of the five climatic oscillations (unfiltered and filtered versions; ENSO is further separated into the CP- and EP-types) in Figure 2, as functions of relative time shift (in months) where positive time shift means the oscillation leading GMSL-ID(t) in phase.

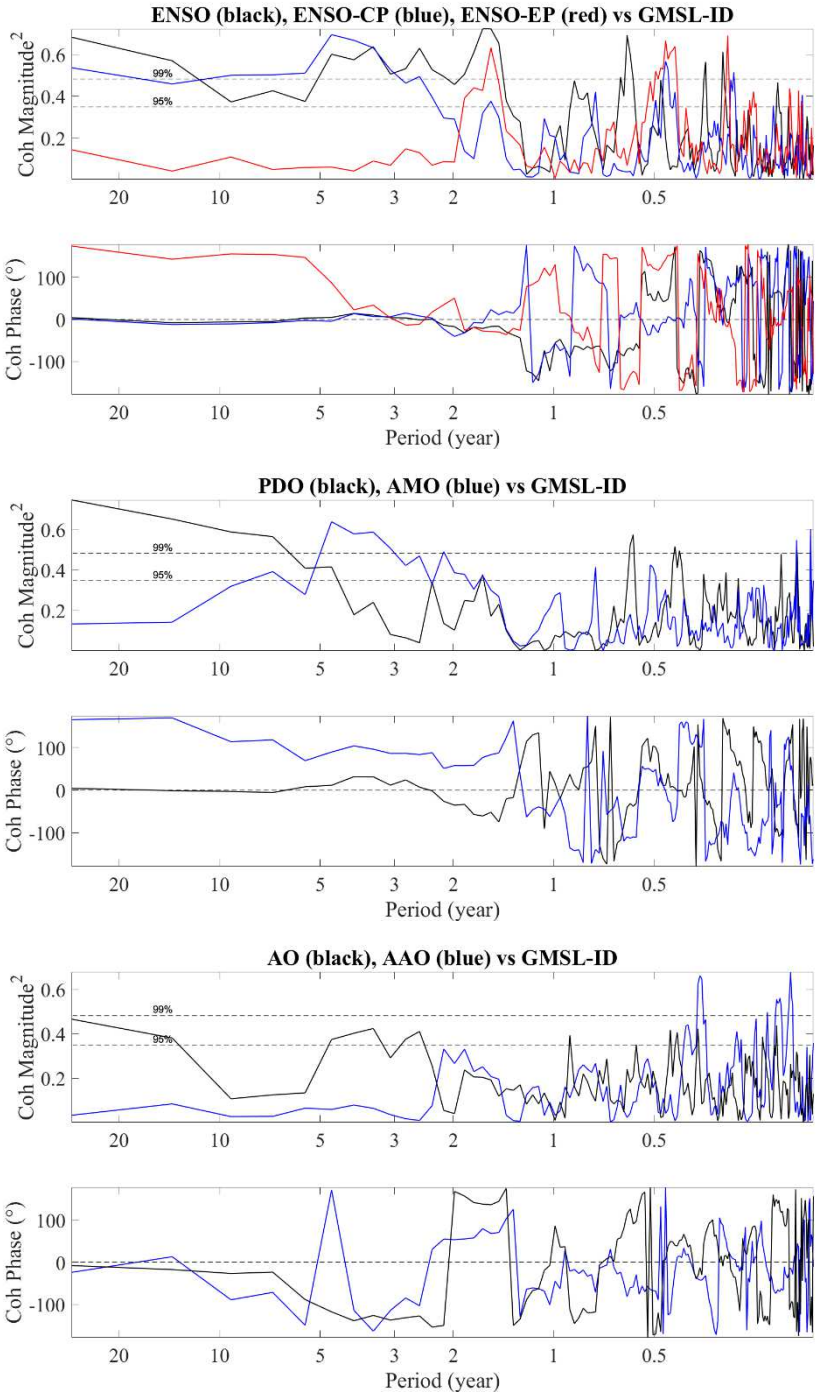

Figure 4. The frequency-domain cross-coherence spectra (magnitude squares and phase) of GMSL-ID(t) w.r.t. the Indices of the five climatic oscillations in Figure 2 as a function of period (in years), where positive phase means GMSL-ID(t) leading: (a) for ENSO (black), ENSO-CP (blue), and ENSO-EP (red); (b) PDO (black) and AMO (blue); (c) AAO (black) and AO (blue). The dashed horizontal lines indicate the statistical confidence levels.

We next conduct a time-domain least-squares fit to GMSL-ID(t) of the five climatic oscillations (filtered version of ENSO and PDO) in linear combination of Indices of the form:

$$\text{GMSL-ID}(t) = k_{\text{ENSO}}*\text{ENSO} + k_{\text{AMO}}*\text{AMO} + k_{\text{PDO}}*\text{PDO}(t) + k_{\text{AAO}}*\text{AAO}(t) + k_{\text{AO}}*\text{AO}(t) + \textit{Residual}(t). \quad (2)$$

We choose to take ENSO MEI to represent the overall ENSO, in lieu of the CP-type and EP-type separately because of the considerable (negative) correlation (−0.47) found between them that makes them unconducive for fitting. AMO and AO indices are time shifted by 8 and 14 months respectively in light of the cross-correlation and cross-coherence found in Figures 3 and 4. The least-squares (by minimizing the variance of *Residual*) estimated coefficients k's give the individual contributions to GMSL-ID(t) per unity of the respective Index value. The fit results are: k_{ENSO} = 1.04, k_{AMO}= −5.59, k_{PDO}= 4.22, k_{AAO}= 0.367, k_{AO} = 0.451. These numbers when normalized by their respective standard deviations become k_{ENSO} = 0.862, k_{AMO}= −0.892, k_{PDO}= 2.55, k_{AAO}= 0.353, k_{AO} = 0.447, which thus indicate the relative importance of each oscillation in contributing to GMSL-ID(t). See Section 4 for ensuing discussions.

4. Discussion and Conclusions

The global mean sea level varies on all timescales for various geophysical reasons. Using satellite altimetry data since 1992, we investigate the influences of the climatic oscillations on global mean sea level on interannual-decadal timescales (GMSL-ID), via correlation analyses of GMSL-ID with the major climatic oscillations in the atmosphere-ocean system: ENSO (CP-type and EP-type), PDO, AMO, AO, and AAO. GMSL-ID is obtained upon removing from GMSL the least-squares estimates of the dominant seasonal and secular trend signals. The latter (at the nominal rate of +3.28 mm/year) is modeled only as a linear slope as opposed to an accelerating, quadratic trend (cf. Yi et al., 2017) that, as we found (results not shown here), would unduly absorb some of the sought climatic influences.

The correlation results are given in Figures 3 and 4. Significant correlations are found for GMSL with ENSO, PDO (low-pass filtered at 8 years), and AMO (with 8-month lag) on respective timescales. In particular, the high GMSL-ENSO correlation coefficient (at essentially zero time-shift) is seen primarily in the CP type but little in the EP type, consistent with the finding of Kuo et al. (2021) and indicating the ENSO-CP's influence of the ocean mixed-layer temperature as well as land-ocean distribution of precipitation mentioned in Section 1. The 8-month lag of AMO might be related to the PDO-AMO relationship, in light of the 1-year lag of AMO relative to PDO reported by Wu et al. (2011).

The lack of GMSL-AAO correlation, which presumably implies that Antarctica continent's land

ice mass melting does not follow AAO in a linear fashion. On the other hand, the lack of significant GMSL-AO correlation (or at most a weak correlation of AO at a 14-month lag to GMSL-ID) warrants further mention: Excluding the Arctic Ocean (above the 66°N latitude), our GMSL data (including the seasonality and trend) would actually reflect any water exchanges of Arctic Sea with the rest of the oceans. Prandi et al. (2012; see also Cheng et al., 2015) estimated the sea level variations of the Arctic Sea (from multi-satellite altimetry), and found no correlation with climatic indices; our present result is consistent with theirs. In this regard, our results are also consistent with a finding by Chao et al. (2020), that it is the atmospheric, not the oceanic, mass transports that are responsible for the intra-seasonal to interannual (non-seasonal) ΔJ_2 associated with AAO and AO variability.

Figure 5 presents the comparison of GMSL-ID(t) with the least-squares combination (2) of the five oscillations, in terms of time series (6a) and frequency-domain coherence spectrum (6b). The good agreement is evident; the time-domain broad-band correlation is as high as 0.86, with extremely high confidence level (cf. Chao & Chung, 2019). The frequency-domain coherence between them resides broadly well over 99% confidence level on interannual timescales longer than ~1.5 years, indeed those targeted in the present study, with zero coherence phase (after the time shifts performed in AMO and AO said above).

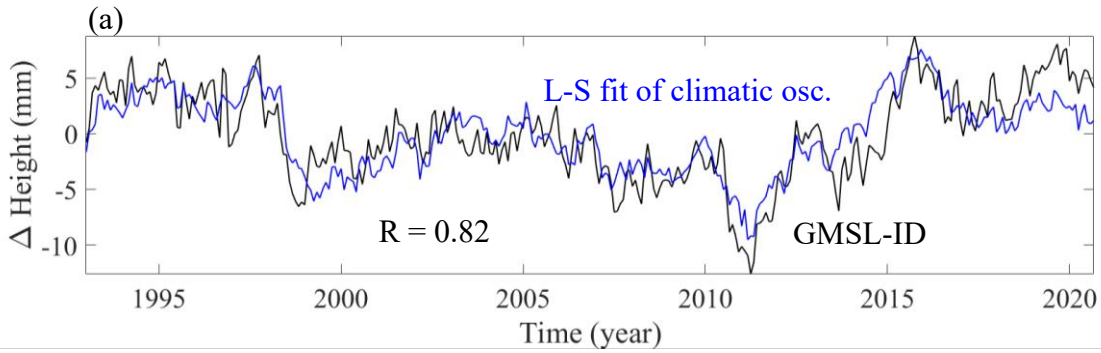

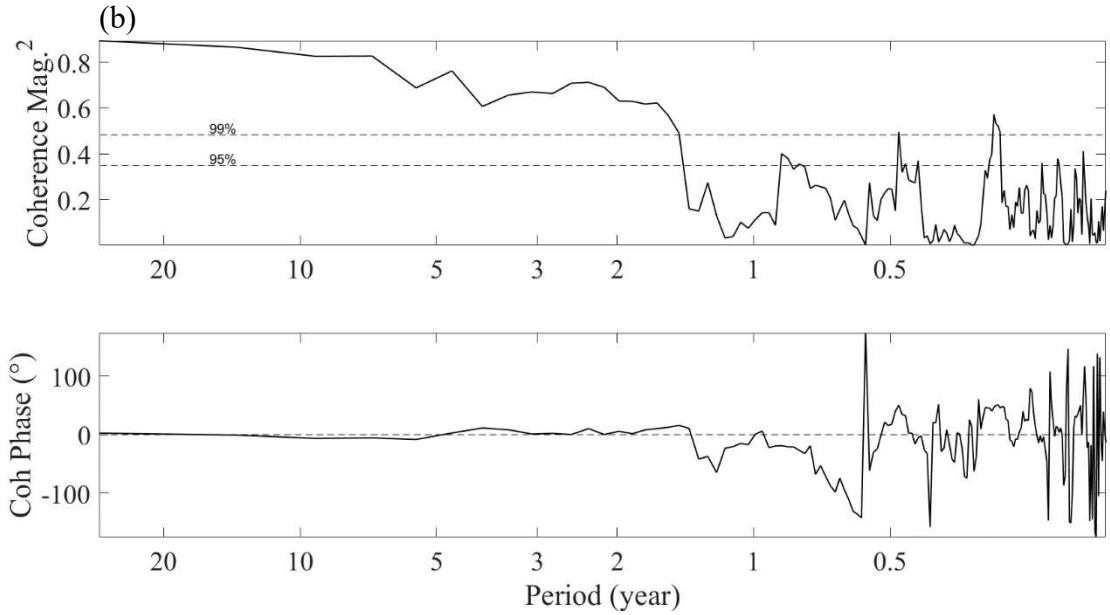

Figure 5. (a) Comparison of GMSL-ID(*t*) (black curve) with the least-squares linear combination of the five oscillation indices (blue curve). (b) Cross-coherence spectrum between the two time series in (a) in terms of magnitude-squared and phase (similar to Figure 4).

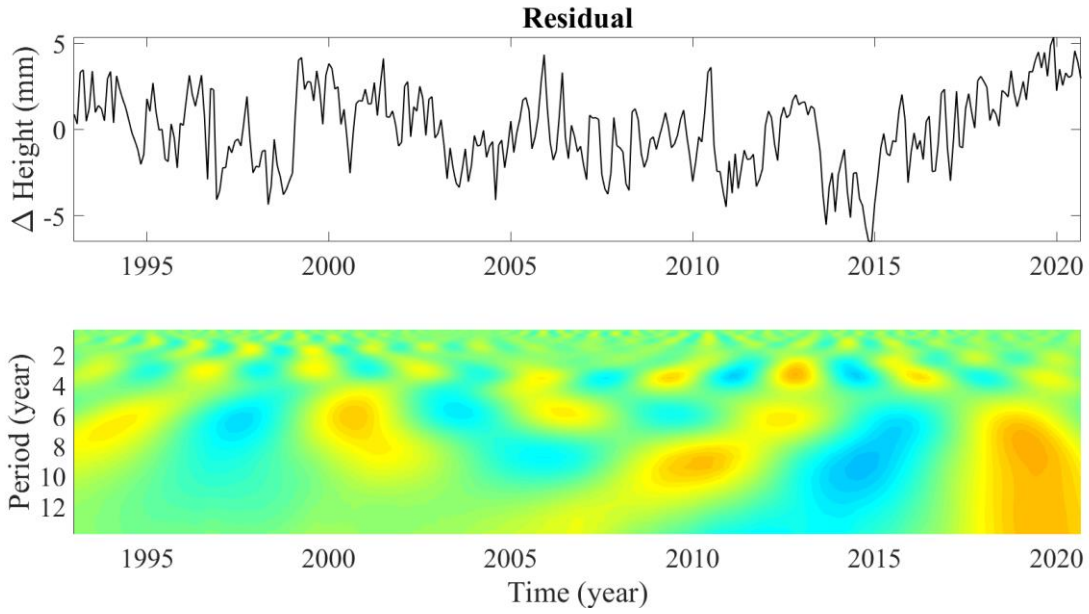

Figure 6. The *Residual* (in Equation 2) time series after the least-squares fit of the five climatic oscillations is removed from GMSL-ID(*t*), i.e. the difference between the two curves in Figure 5(a), along with its time-frequency Morlet wavelet spectra.

The consequent *Residual*(*t*) time series (in Equation 2) is plotted in Figure 6 along with its wavelet spectra. It represents the remnant after the optimal combination of the known climatic oscillation effects are removed from GMSL. Now buried in relatively high noises, it in principle contains signals missed or unaccounted for by the major climatic oscillations, presumably including anthropogenic influences from artificial reservoirs water impoundment (Chao et al., 2008) and underground water withdrawal (Wada et al., 2012).

Our treatment of the climatic influences in terms of indices does not distinguish between the steric- and the mass-induced effects, the two main contributions to GMSL variations. To that end in pursuit of more insights into the responsible mechanisms, one would resort to additional global data types than the present ocean altimetry. A general prospective practice is to combine the GRACE satellite time-variable gravity data such as in Llovel et al. (2010) and Kuo et al. (2021) along with other types of in situ data or numerical model output.

List of abbreviations

GMSL: Global Mean Sea Level

GMSL-ID: Interannual-Decadal Variation of GMSL

ENSO: El Niño-Southern Oscillation

ENSO-CP: Central Pacific ENSO

ENSO-EP: Eastern Pacific ENSO

PDO: Pacific Decadal Oscillation

AMO: Atlantic Multidecadal Oscillation

AO: Arctic Oscillation

AAO: Antarctic Oscillation

Ethics approval and consent to participate

Not applicable

Consent for publication

Not applicable

Availability of data and material

The following organizations provided the datasets used in this paper: sea level data from: https://sealevel.colorado.edu/data/2020rel1-global-mean-sea-level-seasonal-signals-retained;

ENSO: https://psl.noaa.gov/enso/mei/; PDO: https://www.ncdc.noaa.gov/teleconnections/pdo/; AMO: https://psl.noaa.gov/data/timeseries/AMO/; AO: https://www.ncdc.noaa.gov/teleconnections/ao/; AAO: https://www.cpc.ncep.noaa.gov/products/precip/CWlink/daily_ao_index/aao/aao.shtml.

Competing interests

There are no known competing interests.

Funding

This work is supported by the Taiwan Ministry of Science and Technology under grant #109-2116-M-001028.

Authors' contributions

The first author TJL performed all the data acquisition, processing and analysis, and the production of figures. The corresponding author BFC initiated the topic, designed the methodology and procedure, and wrote the paper.

Acknowledgments.

This work was conducted under the first author JTL's science project at the Affiliated Senior High School of National Taiwan Normal University sponsored by Taiwan Ministry of Education.

References

Armitage T, Bacon S, Kwok R (2018) Arctic Sea Level and Surface Circulation Response to the Arctic Oscillation, Geophysical Research Letters, 45, 6576-6584.

Boening C, Willis JK, Landerer FW, Nerem RS, Fasullo J (2012) The 2011 La Niña: So strong, the oceans fell, Geophysical Research Letters, 39.

Carret A, Johannessen JA, Andersen OB, Ablain M, Prandi P, Blazquez A, Cazenave A (2017) Arctic Sea Level During the Satellite Altimetry Era. Surv Geophys 38**,** 251–275. Doi: 10.1007/s10712-016-9390-2

Cazenave A, Henry O, Munier S, Delcroix T, Gordon AL, Meyssignac B, Llovel W, Palanisamy H, Becker N (2012) Estimating ENSO Influence on the Global Mean Sea Level, 1993-2010, Marine Geodesy, 35, 82-97. doi: http://dx.doi.org/10.1080/01490419.2012.718209.

Cazenave A, The WCRP Global Sea Level Budget Group (2018) Global sea-level budget 1993–present, Earth Syst. Sci. Data*, 10*, 1551-1590, doi: https://doi.org/10.5194/essd-10-1551-2018.

Cazenave A, Remy F (2011) Sea level and climate: measurements and causes of changes, Wiley Interdiscip. Rev.-Clim.Chang., 2(5), 647-662, doi: http://dx.doi.org/10.1002/wcc.139.

Chambers DP, Mehlhaff CA, Urban TJ, Fujii D, Nerem RS (2002) Low-frequency variations in global mean sea level: 1950-2000, Journal of Geophysical Research-Oceans, 107(C4), 3026, doi: http://dx.doi.org/10.1029/2001JC001089.

Chao BF (1988) Correlation of interannual length-of-day variation with El Niño / Southern Oscillation, 1972-1986. Journal of Geophysical Research: Solid Earth, 93(B7), 7709-7715.

Chao BF, Chung CH (2019) On Estimating the Cross-Correlation and Least-squares Fit of One Dataset to Another with Time Shift, Earth Space Science, doi: 10.1029/2018EA000548.

Chao BF, Chung WY, Shih WY, Hsieh YK (2014) Earth's rotation variations: A wavelet analysis, Terra Nova, 26, 260-264, doi: 10.1111/ter.12094.

Chao BF, Eanes RJ (1995) Global gravitational change due to atmospheric mass redistribution as observed by the Lageos' nodal residual, Geophysical Journal International. *122*, 755-764.

Chao, BF, Wu YH, Li YS (2008) Impact of artificial reservoir water impoundment on global sea level, Science, doi: 10.1126/science.1154580.

Chao BF, Yu Y, Chung CH (2020) Variation of Earth's Oblateness J_2 on Interannual-to-Decadal Timescales, J. Geophysical Research Letters, *125*, doi: 10.1029/2020JB019421.

Chen JL, Wilson CR, Tapley BD, Famiglietti JS, Rodell M (2005) Seasonal global mean sea level change from satellite altimeter, GRACE, and geophysical models, J. Geod., 79, 532– 539, DOI: 10.1007/s00190-005-0005-9.

Cheng YC, Andersen O, Knudsen P (2015) An Improved 20-Year Arctic Ocean Altimetric Sea Level Data Record, Marine Geodesy, 38(2), 146-162, doi: https://doi.org/10.1080/01490419.2014.954087

Ding H, Chao BF (2018) Application of stabilized AR-*z* spectrum in harmonic analysis for geophysics, Journal of Geophysical Research, doi: 10.1029/2018JB015890

Frederikse T, Landerer F, Caron L, Adhikari S, Parkes D, Humphrey VW, Dangedorf S, Hogarth P, Zanna L, Cheng L, Wu YH (2020) The causes of sea-level rise since 1900. Nature 584, 393–397, https://doi.org/10.1038/s41586-020-2591-3

García-García D, Vigo I, Trottini M (2020) Water transport among the world ocean basins within the water cycle, Earth Syst. Dynam., 11, 1089–1106, https://doi.org/10.5194/esd-11-1089-2020

Haddad M, Taibi H, Arezki SMM (2013) On the recent global mean sea level changes: Trend extraction and El Nino's impact, Comptes Rendus Geoscience, 345(4), 167-175, doi: http://dx.doi.org/10.1016/j.crte.2013.03.002.

Hamlington BD, Leben RR, Strassburg MW, Nerem RS, Kim, K. (2013). Contribution of the Pacific Decadal Oscillation to global mean sea level trends. Geophysical Research Letters, 40(19), 5171-5175. doi:10.1002/grl.50950

Hamlington BD, Reager JT, Lo M, Karnauskas KB, Leben RR. (2017). Separating decadal global water cycle variability from sea level rise. Scientific Reports, 7(1). doi:10.1038/s41598-017-00875-5

Hamlington BD, Piecuch CG, Reager HT, Chandanpurkara H, Frederiksea T, Nerem RS, Fasullo JT, Cheon SH (2019) Origin of interannual variability in global mean sea level. doi: 10.1073/pnas.1922190117

Jin TY, Li JC, Jiang WP, Chu YH (2012) Low-frequency sea level variation and its correlation with climate events in the Pacific, Chinese Science Bulletin, 57(27), 3623-3630, doi: http://dx.doi.org/10.1007/s11434-012-5231-y.

Kuo YN, Lo MH, Liang YC, Tseng YH, Hsu CW (2021) Terrestrial Water Storage Anomalies emphasize interannual variations in global mean sea level during 1997–1998 and 2015–2016 El Niño events. Geophysical Research Letters, 48(18). https://doi.org/10.1029/2021gl094104

Llovel W, Becker M, Cazenave A, Cretaux JF, Ramillien G (2010) Global land water storage change from GRACE over 2002-2009; Inference on sea level, Comptes Rendus Geoscience, 342(3), 179-188, doi: http://dx.doi.org/10.1016/j.crte.2009.12.004.

Prandi P, Ablain M, Cazenave A, Picot N (2012) A New Estimation of Mean Sea Level in the Arctic Ocean from Satellite Altimetry, Marine Geodesy, 35, 61-81, doi: http://dx.doi.org/10.1080/01490419.2012.718222.

Rasmusson EG, Carpenter TH, (1982) Variations in tropical sea surface temperature and surface wind fields associated with the Southern Oscillation/El Niño. Mon. Wea. Rev., 110, 354-384.

Rohmer J, Cozannet LG (2019) Dominance of the mean sea level in the high-percentile sea levels time evolution with respect to large-scale climate variability: a Bayesian statistical approach, Environ. Res. Lett. 14, 014008

Thompson DWJ, Wallace JM (2000) Annular Modes in the Extratropical Circulation. Part I: Month-to-Month Variability, Journal of Climate, https://doi.org/10.1175/1520-0442.

Vinogradov SV, Ponte RM, Heimbach P, Wunsch C (2008) The mean seasonal cycle in sea level estimated from a data-constrained general circulation model, Journal of Geophysical Research, 113, C03032, doi:10.1029/2007JC004496.

Wada Y., van Beek LPH, Weiland FCS, Chao BF, Wu YH, Bierkens MFP (2012) Past and future contribution of global groundwater depletion to sea-level rise, *Geophys. Res. Lett.*, *39*, L09402, doi:10.1029/2012GL051230.

Wahl T, Chambers DP (2016) Climate controls multidecadal variability in US extreme sea level records Journal of Geophysical Research-Oceans 121 1274–90, https://doi.org/10.1002/2015JC011057

Wallace JM, Gutzler DS (1981) Teleconnections in the geopotential height field during the northern hemisphere winter. Monthly Weather Review, 109(4), 784– 812.

Willis JK, Chambers DP, Nerem RS (2008) Assessing the globally averaged sea level budget on seasonal to interannual timescales, Journal of Geophysical Research-Oceans, 113(C6), C06015, doi: http://dx.doi.org/10.1029/2007JC004517.

Wu S, Liu Z, Zhang R, Delworth TL (2011) On the observed relationship between the Pacific Decadal Oscillation and the Atlantic Multi-decadal Oscillation. Journal of Ocean 67, 27–35. https://doi.org/10.1007/s10872-011-0003-x

Volkov DL, Landerer FW (2013) Nonseasonal fluctuations of the Arctic Ocean mass observed by the GRACE satellites. Journal of Geophysical Research-Oceans, 118, 6451– 6460.

Yi S, Heki K, Qian A (2017) Acceleration in the Global Mean Sea Level Rise: 2005-2015, Geophysical Research Letters, 44(23), 11905-11913. https://dx.doi.org/10.1002/2017gl076129.

Yu JY, Kao HY (2007) Decadal changes of ENSO persistence barrier in SST and ocean heat content indices: 1958–2001, Journal of Geophysical Research, 112, D13106, doi:10.1029/2006JD007654.

Zhang XB, Church JA (2012) Sea level trends, interannual and decadal variability in the Pacific Ocean, Geophysical Research Letters, 39(21), L21701, doi: http://dx.doi.org/10.1029/2012GL053240.